

THE LAKE TELETSK TECTONIC DEPRESSION (ALTAI): NEW KINEMATIC DATA AND CHRONOLOGICAL RELATIONS

B. Dehandschutter¹, D. Delvaux¹, A. Boven²

¹Royal Museum of Central Africa, Department of Geology and Mineralogy, B-3080 Tervuren.

²Vrije Universiteit Brussel, Department Geologie, Pleinlaan 2, B-1050 Brussel, Belgium

Abstract. - Lake Teletsk, situated at the northern end of the Central-Asian fold belt, in Altai, South Siberia, is a long, narrow and deep basin, surrounded by steep slopes which extend the basin up to 2800 meters. The lake is situated at the contact zone between two different geodynamic terrains. Analysis of the brittle structures, using remote sensing techniques together with field investigations, paleostress reconstructions and joint set analysis, revealed new indications on the tectonic nature of the Lake Teletsk graben. The collapse of the basin seems to be a very young process (less than 1 Ma). It appears that many of the recent structures evolved along pre-existing weakness zones, comprising a mylonitic shear zone and a suture zone.

⁴⁰Ar/³⁹Ar step-wise heating results on two biotite and one amphibole separate from mylonitized gneisses belonging to the shear zone, yield concordant apparent plateau cooling ages of 380 ± 5 Ma, suggesting rapid cooling. This timing corresponds to the emplacement of the granite-gneiss domes. Another sample of a mylonitized gneiss belonging to the same unit, however distinctly enriched in amphibole blasts, yields a discordant amphibole age spectrum with an average apparent plateau age of 260 ± 7 Ma. This age is thought to reflect a ductile shear event associated to the Permian thrust and strike-slip faulting, formerly described for the Teletsk region. Brittle reactivation appears to be limited to narrow zones and remains so far undated.

Paleostress reconstructions allowed to differentiate three different stress states in the Teletsk Lake area. A first Paleozoic phase is post-ductile, while a last phase was active during the late Quaternary. The timing of the second tectonic phase remains uncertain, because of the limited amount of available constraining relations.

Résumé. - Le lac Teletsk est situé à la limite nord de l'orogène de l'Asie Centrale, au sud de la Sibérie. Il s'agit d'un graben long, étroit et profond. Le bassin est bordé par des flancs redressés, surmontant le lac jusqu'à 2800 m. Le lac se trouve dans la zone de contact entre deux blocs géodynamiques. L'analyse des structures cassantes par télédétection, investigation du terrain et reconstitution des paléocontraintes apporte de nouvelles indications sur l'origine tectonique récente du bassin. Il apparaît que beaucoup de structures récentes se sont développées le long de zones faibles préexistantes, comprenant une zone mylonitique et une suture.

Dans le contexte tectonique général, une étude géochronologique des structures ductiles est réalisée. Le métamorphisme gneissique dans le Dévonien inférieur serait âgé de 380 ± 5 Ma; il serait suivi par une phase de réchauffement local au Permien datée à 260 ± 7 Ma. L'âge dévonien limite la tectonique cassante. Une reconstitution des paléocontraintes permet de différencier trois phases de contrainte; la première est d'âge paléozoïque et la dernière d'âge quaternaire. La datation de la deuxième phase est compliquée par l'absence d'une séquence stratigraphique complète dans les structures liées à cette phase. Les différentes possibilités sont présentées.

Samenvatting. - Het Teletsk meer bevindt zich aan de noordelijke rand van het Centraal-Aziatische plooigebied, in Altai, Zuid Siberië. Het is een lang, smal en diep extensiebekken, omringd door steilranden die tot 2800 m boven het bekken uitsteken. Het meer bevindt zich in de contactzone tussen twee geodynamische blokken. Analyse van de breukstructuren aan de hand van teledetectie, veldwerk en paleostress reconstructies, leidde tot nieuwe aanwijzingen voor de tectonische oorsprong van het bekken. Ook werd er aangetoond dat veel van de

recente structuren ontstonden langsheen vóórbestaande zwaktezones, zoals een mylonitische shearzone en een sutuur zone.

In een meer algemeen tektonisch kader werd een geochronologische studie van de ductiele structuren in de sokkel uitgevoerd. Dit leidde tot de datering van het metamorfisme dat leidde tot de gneiss-vorming (in het Onder Devoon, 380 ± 5 Ma) en van een lokale fase van opwarming (in het Onder Perm, 260 ± 7 Ma). Deze datering leidde ook tot de tijdsbegrenzing van de breuktectoniek. Een paleostress reconstructie werd ook uitgevoerd, waardoor de oriëntatie van de spanningsellipsoïde, die aan de oorzaak van de breukbeweging ligt, bepaald werd. Er werden drie verschillende spanningsfasen onderscheiden, waarvan de eerste van Paleozoische ouderdom is, en de laatste van Kwartaire ouderdom. De tweede fase, die tevens de meest uitgesproken is, is niet eenduidig te dateren, omwille van het ontbreken van stratigrafische controles in de structuren die met deze fase zijn geassocieerd. Verschillende mogelijkheden voor de betekenis van deze fase worden besproken.

1. INTRODUCTION

The Teletsk Lake depression (fig. 1) is a long (80 km), narrow (average of 4 km) and deep (~ 300 m of water, ~ 1000 m of sediments) sedimentary basin, located at the northwestern extremity of the Altai-Sayan foldbelt, in the Autonomous Republic of Gorny-Altai, South Siberia. This region forms part of the Central

Asian orogenic belt, which is composed of different block units. These blocks were formed during early Palaeozoic to each other along transverse fault zones during the whole Palaeozoic (Dergunov accretion- collisional tectonics, and underwent important displacement relative, 1979; Mossakovski and Dergunov, 1985; Suess, 1901; Berzin *et al.*, 1994; Buslov and Sintubin, 1995).

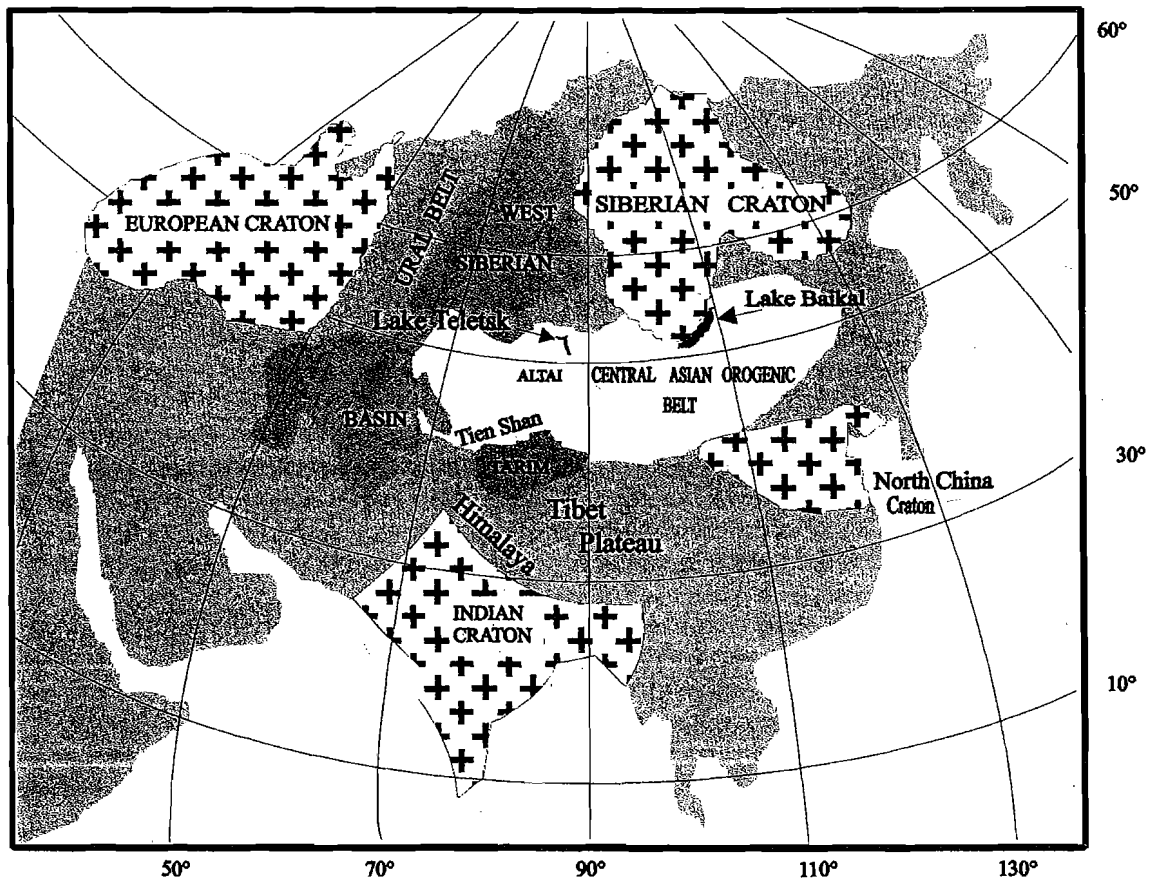


Fig. 1. – Localisation of Lake Teletsk in Altai, Central Asia, South Siberia. The Central Asian orogenic belt is situated between the stable cratons. The principal geographic regions are indicated.

Lake Teletsk is situated along the contact zone between two such blocks: the *West-Sayan* and the *Gorny-Altai* geodynamic terrains (fig. 2). Cenozoic tectonic activity within the region mainly occurred by reactivation of the older structures. According to Molnar and Tapponnier (1975) the driving force for the Cenozoic tectonic shortening of Central Asia and for (re)activation of the (pre-existing) structures is the Indo-Eurasian convergence.

For the whole Central Asian fold belt, an active strike-slip stress regime was derived from earthquake focal mechanism and fault geometry (Dergunov, 1972; Molnar and Tapponnier, 1975; Tapponnier and Molnar, 1979; Cobbold and Davy, 1988; Abrakhmatov *et al.*, 1996). Neotectonic stress determination from brittle fault slip data later brought into detail the local stress fields in various parts of the Central Asian fold belt (Delvaux *et al.*, 1995b).

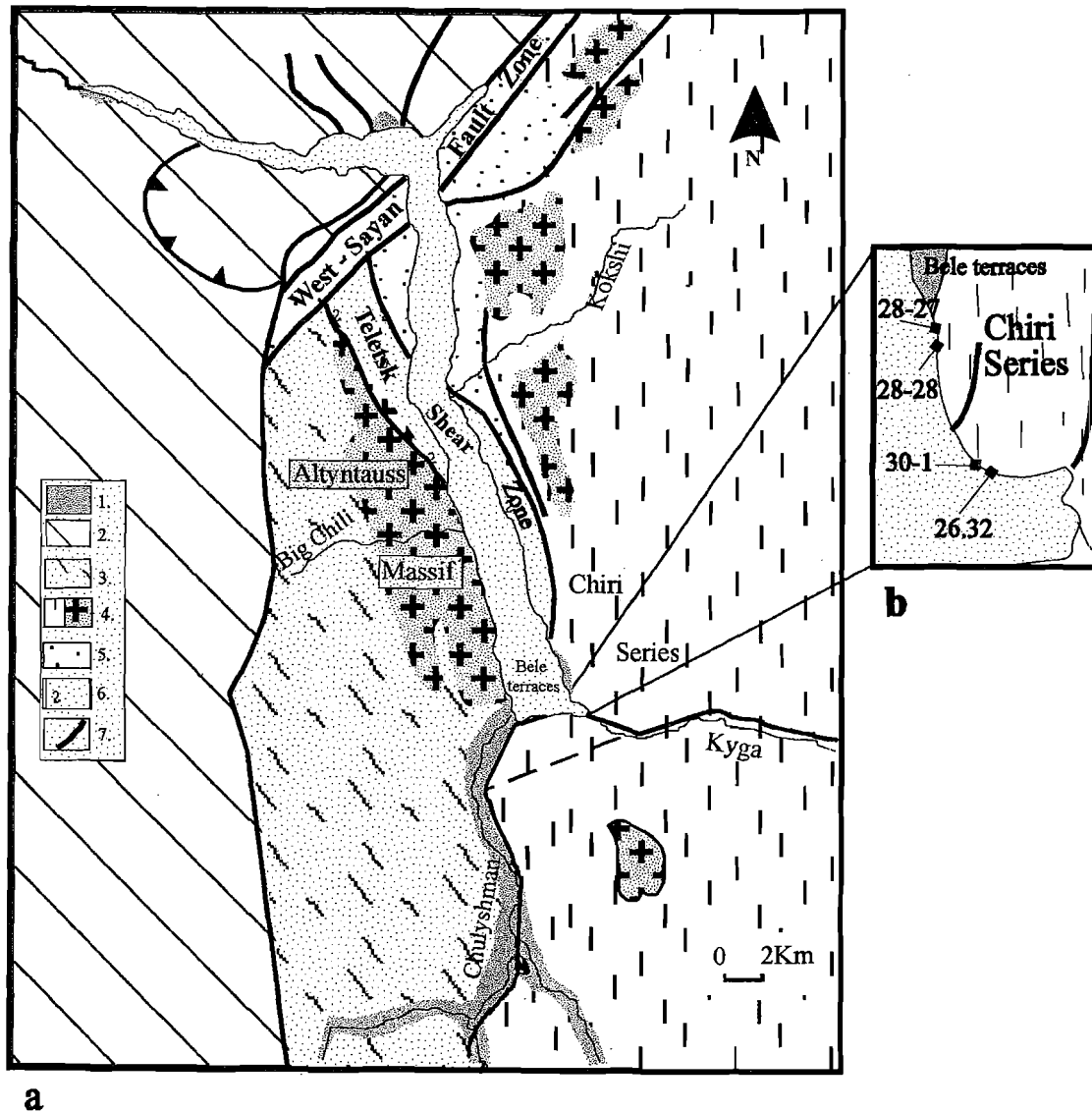


Fig. 2. - Geology and Structural Elements of Teletsk Lake area. (a) Geology of the Teletsk lake (after Buslov *et al.*, 1993); (b) Location of Ar-Ar sampling sites.

1. Quaternary sediments. 2. Gorny-Altai terrain: Proterozoic and Paleozoic island arc rocks. 3-5, West-Sayan terrain: 3. Vendian Amphibolites; 4. Lower Paleozoic Granite-Gneiss domes; 5. Lower Paleozoic Greenschists. 6. Teletsk Shear zone: Mylonites. 7. Strike-slip faults.

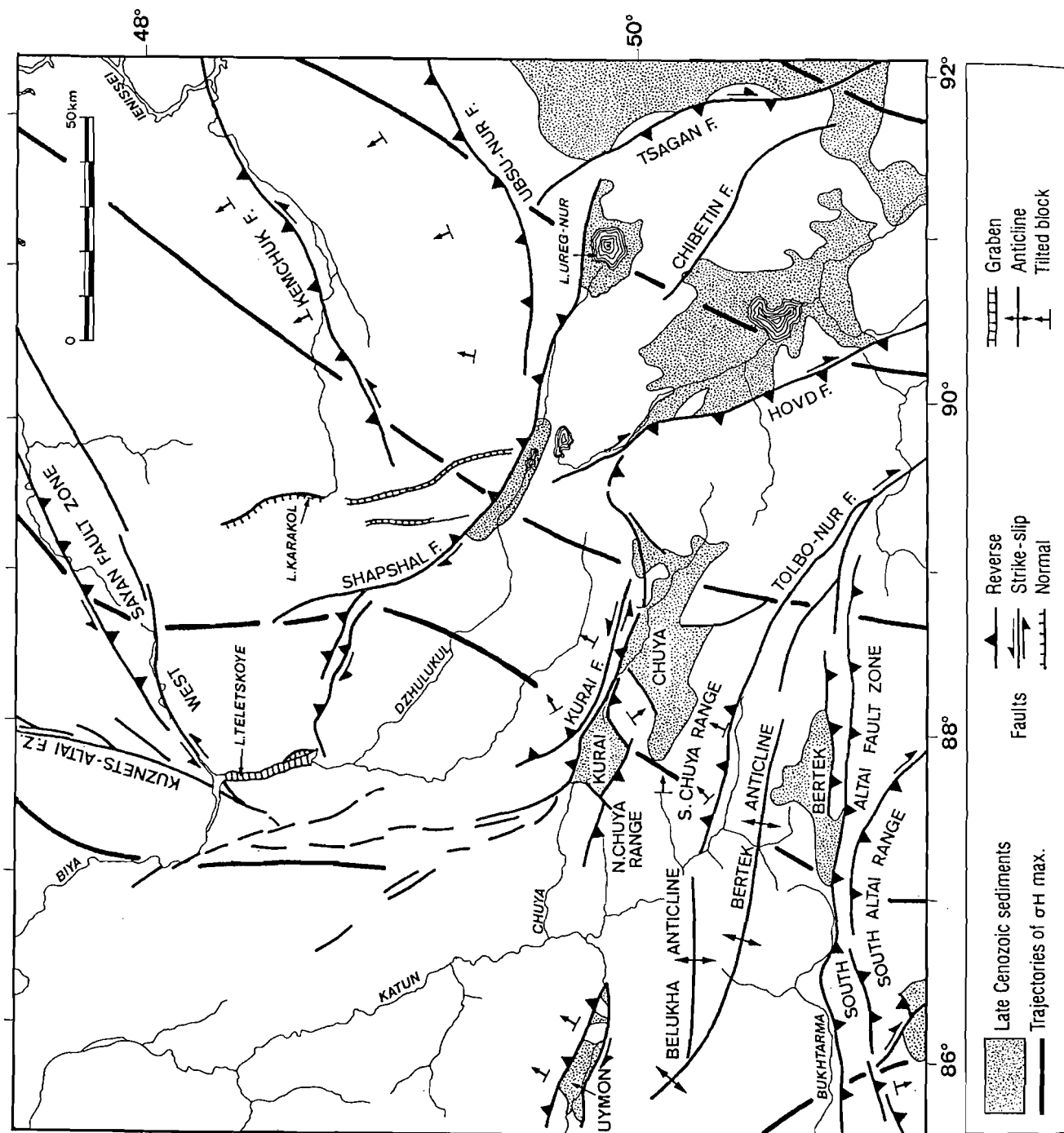


Fig. 3. - Cenozoic kinematics of north-east Altai. Indicated are the major active faults with their kinematics. Normal faults generally show a submeridional trend. Reverse faults and thrusts mostly show a lateral trend. Strike-slip faults trend obliquely. The direction of block tilts is mainly towards the north or northeast. The direction of the principal horizontal compression varies from submeridional in the south to a NE direction towards the north. The direction of block tilting is mainly towards the north or northeast. The direction of the principal horizontal compression varies from submeridional in the south to a NE direction towards the norths.

The tectonic nature of the Teletsk Lake depression was proposed by several scientists since the beginning of this century, and has been reviewed by Dergunov (1972) and Lukina (1991). These authors noticed the peculiar morphology of the basin, the steep and high slopes and the high water depth. They also recognised several active fault zones, partly controlled by old strike-slip fault zones and suture zones, located between the Palaeozoic terrains. In order to contribute to the understanding of the general tectonic evolution of the Teletsk region, four samples of the ductile basement in the south-eastern part of the lake have been studied using the stepwise heating ^{40}Ar - ^{39}Ar technique. In the same tectonic framework, a study of the brittle structures around the lake was carried out. This comprised paleostress analysis, joint set analysis and morpho-structural analysis of satellite images and aerial photographs.

2. GEOLOGICAL AND GEODYNAMICAL SETTINGS

Teletsk Lake is situated at the western extremity of the *West-Sayan terrain* (fig. 2). This block is characterised by Upper Proterozoic amphibolites and ophiolitic complexes, overlain by early Palaeozoic metamorphic sediments (greenschist facies) and intruded by Devonian granite-gneiss domes. In the northern part of the lake the *Gorny-Altai terrain* crops out. This terrain is composed of tholeiitic basalts covered by early Palaeozoic molasse sediments. Both terrains have supposedly been formed during the geodynamic evolution of the Palaeo-Asian Ocean (Dobretsov *et al.*, 1995a). In this view, the Gorny-Altai terrain was formed by Vendian island arc magmatism. It underwent severe tectonic deformation during the early Cambrian, when it was deformed into an accretionary wedge. This wedge collided with the Siberian continent at the end of the Cambrian. This resulted in the formation of back- and fore-arc sedimentary basins, filled with the detritus of the accretionary wedge. The West-Sayan block was formed independently during the Precambrian, in a marginal sea environment, which evolved into an active continental margin towards the Devonian, with the intrusion of granitic plutons, reflected by the outcropping granite-gneiss domes.

The contact between the Gorny-Altai terrain and the West-Sayan terrain was not established

until the late Permian, when the whole Altai region was affected by strike-slip deformation along suture zones between the different stable blocks. These movements are related to the final closure of the Palaeo-Asian ocean, with the collision of the Kazakhstan micro-continent and the Siberian (Angara) Craton (Dobretsov *et al.*, 1995a).

The *West-Sayan fault* marks the border between the Gorny-Altai terrain and the West-Sayan terrain. According to Buslov and Sintubin (1995), it originated from thrust and strike-slip movements during the Permian era. This fault zone extends towards the north-east over a distance of more than 1000 km, into the East-Sayan fault, up to the Baikal region. It has a width of about 8 km, and is composed of different blocks, which are horizontally displaced.

The *Teletsk shear zone* crosscuts the West-Sayan block in the Teletsk Lake area. It is composed of mylonitic rocks of Devonian age. To the north, this shearzone is interrupted by the West-Sayan fault zone. Its continuation along the eastern border of the lake remains a topic of discussion. According to Buslov and Sintubin (1995) the Teletsk shear zone curves towards the south. All structural units within the shear zone display a gentle dip to the east. It is therefore interpreted as a former thrust zone, along which rocks were pushed from the east onto the western Teletsk metamorphic complex. This complex is composed of Vendian amphibolites, intruded by Devonian granitoids of the Altyntauss massive. These granitoids display a contact metamorphic aureole characterised by gneisses and quartz-granite-muscovite schists (Buslov and Sintubin, 1995). The Teletsk metamorphic complex is situated between Lake Teletsk and the western border of the West-Sayan terrain (fig. 2). Comparable Devonian granitoids outcropping as domes occur to the east of the Teletsk shear zone. They are surrounded by the paragneissic zone of the Chiri series, metamorphosed under amphibolite facies conditions.

3. CENOZOIC TECTONICS

3.1. The Altai Region

The Altai region, and Central Asia in general, is characterised by a high seismicity and by a complex mosaic structure of tectonic blocks of

different elevations, separated dominantly by wrench fault zones.

The general aspects of the present-day structural geometry in Altai are NW and SE striking transverse faults, lateral striking thrust to thrust-oblique (i.e. with a strike-slip component) and *reverse* faults, NS trending normal faults and elongated graben structures (fig. 3; Dergunov, 1972; Dobretsov *et al.*, 1995b).

The recent deformation occurs preferentially along the old sutures between the different geodynamic complexes of the basement. This is because such zones are lithospheric zones of weakness, most susceptible for stress induced strain.

The studies of the stress distribution derived from earthquake focal mechanisms (Cobbold and Davy, 1988), fault geometry (Tapponnier and Molnar, 1979) and paleostress reconstructions from fault slip data in Quaternary sediments (Delvaux *et al.*, 1995b) show that, in the Central Asian region, the horizontal principal compressive stress has a fan shape with orientations ranging from NW-SE in south Altai (Zaisan area) over N-S in north Altai (West-Sayan), to NE-SW in East-Sayan.

3.2. The Teletsk area

The Cenozoic tectonic structures in this area appear to be mainly controlled by pre-existing structures (fig. 2). The West-Sayan Fault Zone is such an old structure, now reactivated as a strike-slip fault zone with a sinistral sense of movement. This sense was derived from fault geometry and displacement of delta sediments (Lukina, 1991). The Teletsk shearzone is also overprinted by a Quaternary reactivation. This is expressed by the occurrence of an unconsolidated breccia filling the margins of the zone. The Shapshal fault (fig. 3), with its (probable) termination in the southern part of the lake near the Kyga river, is supposed to have a dextral Quaternary movement (Delvaux *et al.*, 1995a).

These structures were considered by various authors to be important for the formation of the lake. Lukina (1991) explained the formation of the lake by a tectonic process, corresponding to a giant tension gash, developing parallel to the local direction of principal compression. Opening of the lake occurred between the sinistral West-Sayan fault, and the dextral Shapshal fault. In this

situation, the West-Sayan terrain is moving eastwards, away from the Gorny-Altai terrain.

Other authors (Delvaux *et al.*, 1995a) attribute the structural difference between the northern and southern segment of the meridionally trending part of the lake to a counterclockwise rotation of the West-Sayan block, resulting in a faster opening, and therefore in more pronounced extensional structures along the southern part of the lake.

Sedimentological studies of the upper metres of the bottom sediments reveal an average sedimentation rate of about 1 mm a year in the north and 8 mm a year near the Chulyshman delta in the south, according to the concentration of ^{137}Cs in undisturbed sediments (Kalugin *et al.*, 1997). Deep seismic profiling indicates that the sedimentary infill reached a thickness of about 1 km (Seleznyov *et al.*, 1996). Taking an average sedimentation rate of 1 mm/y, these data roughly suggest that sedimentary infill started around 1 Ma, meaning that the initial opening of the lake basin would have occurred around this time.

4. GEOCHRONOLOGY

4.1. Introduction

In order to have a better insight in the tectonic evolution of the Teletsk shearzone (its metamorphism and ductile deformation), radio-isotopic datings were performed on basement rocks. Two sets of biotite and two sets of amphibole were separated from mylonitic gneisses belonging to the Chiri-series in the southeastern part of Lake Teletsk (fig. 2b). These gneisses resulted from metamorphism of terrigenous sediments. This is inferred from the observed preservation of a graded rhythmical bedding in the gneissic rocks. The minerals were analyzed by the step-wise heating ^{40}Ar - ^{39}Ar technique. This method provides insight on the distribution of the argon isotopes within the minerals, and as such allows to assess some information on the thermal evolution which affected the sample during the tectonic and metamorphic events. Both the biotite and the amphibole display a microstructural fabric which is related to the ductile shearing which affected the gneisses belonging to the Chiri-series. In the present case, the dating of the ductile stages provides an upper age limit for brittle tectonics in the rheologically homogeneous region.

4.2. Sample description

The gneiss samples from which amphibole was separated (28-27 and 26-32, see location on fig. 2) show a banded compositional layering of light (quartz, albite) and dark (hornblende, epidote-clinozoisite, sphene) minerals. The mineral association corresponds to the *epidote-amphibolite facies* (upper-amphibolite facies). Both samples display a gneissic texture and a mylonitic strain (since the quartz shows an undulatory extinction and a ribbon structure).

Two types of amphibole are observed in the gneisses: a brownish type, which occurs as small crystals in the fine grained matrix parallel to the foliation (called fabric 1); and a greenish type, composed of bigger grains, showing an oblique orientation with respect to the first type (called fabric 2). The amphiboles of fabric 2 are restricted to narrow zones, independent of the composition of the gneissic layers.

In the samples from which biotite was separated (28-28 and 30-1, see location on fig. 2), a gneissic layering and an amphibolite facies mineral association is also present. The melanocratic bands consist of biotite, without any amphibole or clinozoisite. This indicates that this gneiss is genetically associated to a Ca-poor mother rock. Opaque minerals are present as inclusions in the biotite and in the interstitial phase, where they are probably ilmenite crystals. Zircon occurs in the biotite and chlorite is seen as greenish crystals in the dark bands. According to their fabric, the biotite crystals can be subdivided into two types, similar as for the amphiboles in samples 28-27 and 26-32. The first, fine grained type (fabric 1) has a very regular orientation parallel to the foliation, whereas the bigger biotite grains (fabric 2) are oriented slightly oblique to this direction. In all four samples, the oblique fabric displays a gentle dip to the east.

The light layers consist of quartz, which is deformed into flaser and ribbon structures due to shear strain. Albite (plagioclase) does not seem to be abundant, but is not easily identified, because of its small grain size. Apatite is present as a trace mineral.

In all samples, all minerals are fresh and no alteration to secondary minerals is observed.

4.3. Analytical methods

Two hornblende separates (28.27 and 26.32) and two biotite separates (30.1 and 28.28) were obtained by heavy liquids and magnetic separation. The separates were purified by hand picking, up to a high degree of purity. Important is to note that the mineral separate of sample 28-27 was enriched in hornblende from fabric 2, because of the nature of the selected gneiss samples, here showing a dense zone of amphiboles belonging to fabric 2.

After irradiation along with the biotite standard HBD1 [for which a K-Ar age of 24.21 Ma has been used (Hess and Lippolt, 1993)] Ca- and K-salt monitors, the samples were submitted to a stepwise heating process in a vacuum resistance oven. The ^{40}Ar , ^{39}Ar , ^{38}Ar , ^{37}Ar and ^{36}Ar isotope abundances were determined with a MAP 216 mass spectrometer, through linear extrapolation at time zero of peak intensities obtained during 15 sequential scans. Step-age calculations were made with the J-factor obtained from the measurements on the HBD1 standard. Corrections were made for Ca, K and Cl derived Ar isotopes, mass discriminations, local neutron flux gradients and decay of ^{37}Ar and ^{39}Ar since the time of irradiation. For every sample, two aliquots were measured separately, in order to control the consistency of the results.

4.4. Results

The stepwise heating diagrams are presented on figure 6. They show a good reproducibility for the measurements on two aliquots, except for sample 28-27. Note that this separate consists of a mixture of two fabrics, which could have different ages (cfr. 4.2). All samples present apparent plateau ages, which refer here to the presence of at least two consecutive steps with similar ages which account for more than 40% of released ^{39}Ar . The ratio Ca/K is also provided. Full data are shown on table 3. The four biotite aliquots of samples 28-28 and 30-1, and the two amphibole aliquots of sample 26-32 yield apparent plateau ages of $375-380 \pm 5$ Ma, corresponding to an early Devonian cooling age. The two amphibole aliquots of sample 28-27 have disturbed staircase shaped spectra, indicating the presence of excess argon at the high

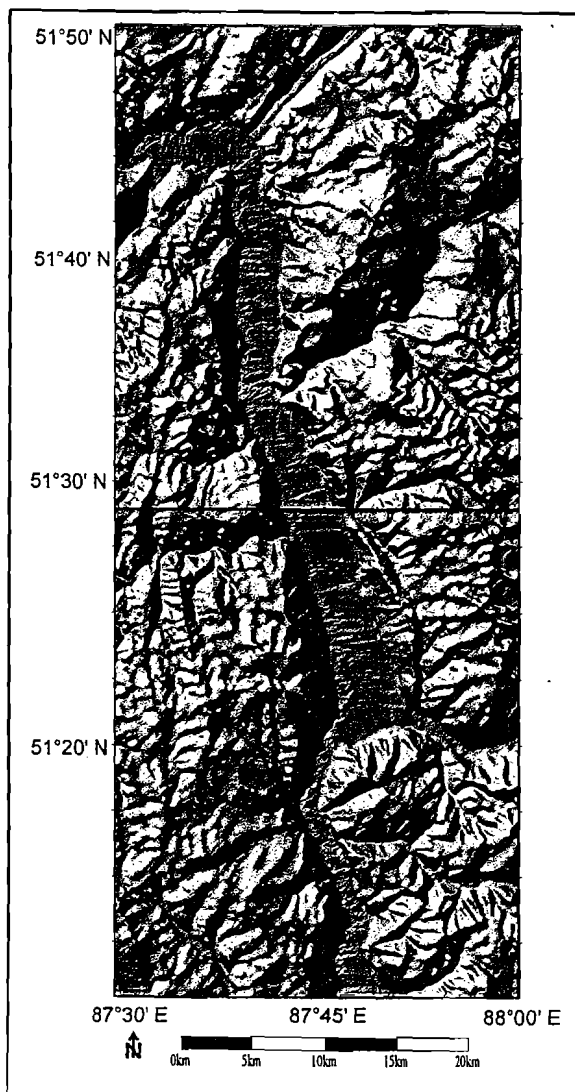


Fig. 4. - Shaded relief DEM of the Teletsk region, showing the main lineament pattern: N40°E trending West-Sayan fault zone in the north; N65°E and N40°W trending lineaments in the south; N10°W trending in the west; curved fault at the southeastern border of the lake, marking the 'loupe' structure.

temperature steps. However, aliquot (a) (fig. 6D) with smaller step age errors shows an apparent plateau age of 236 ± 7 Ma, while aliquot (b) yields a single step age of 274 ± 9 Ma, in average ca 260 ± 7 Ma corresponding to an early Permian cooling age. The Ca/K is very high in sample 28-27. This probably results from the presence of impurities of sphene and epidote-clinozoisite in the amphibole grains.

5. BRITTLE STRUCTURES AROUND THE TELETSK BASIN

5.1. Lineament pattern and field observations

A detailed analysis of MIR and Landsat satellite images and aerial photographs resulted in the mapping of the lineament patterns of the lake area. Stereoscopic investigations recognised (where relevant) the relative displacement along the lineaments. The characteristics of these lineaments were compared to the structures observed in the field (joints, faults, topographic block structures, foliation, terraces,...).

The lineament pattern is characterised by NE, NW and NNE directions for the West-Sayan fault area in the north (figs. 2, 4 and 5). In the middle part of the lake, the NW direction of the Teletsk shearzone is more clearly expressed, with several indications of a possible recent activation of the zone. This is expressed by the presence of a modern block morphology which can be explained as extensional duplexes.

The southwestern area is characterised by a NNW lineament direction, subparallel to the southwestern border of the lake. Closer to the lake, a cross pattern of NE and NW trending lineaments seems to be characteristic, while on the eastern side of the lake, the NE trend is persistent (fig. 5).

In the southwestern part, on the higher elevations of the Altyntauss massif, many submeridional trending oblique faults seem to cut Quaternary glacial deposits, and closer to the shoreline, a system of normal faults, parallel to the shore is observed, towards the south of the Big Chili river. A similar seismo-tectonic line was observed in the northeastern part of the area.

A comparable pattern of faults cutting Pleistocene glacial deposits estimated to be not older than 10^4 years is observed on the higher parts of the eastern ridges (Delvaux *et al.*, 1995a).

In the Altyntauss massif, a series of oblique, NW trending faults are very prominent on aerial pictures, satellite images as well as in outcrop morphology. In general, they have a very steep NE wall, which shows almost over all its length clear indications of strike-slip movements. Most of the SW walls are covered by vegetation, and are far less steep. The expression of these structures is very prominent, and therefore it is associated to major recent tectonic events. The very fresh state

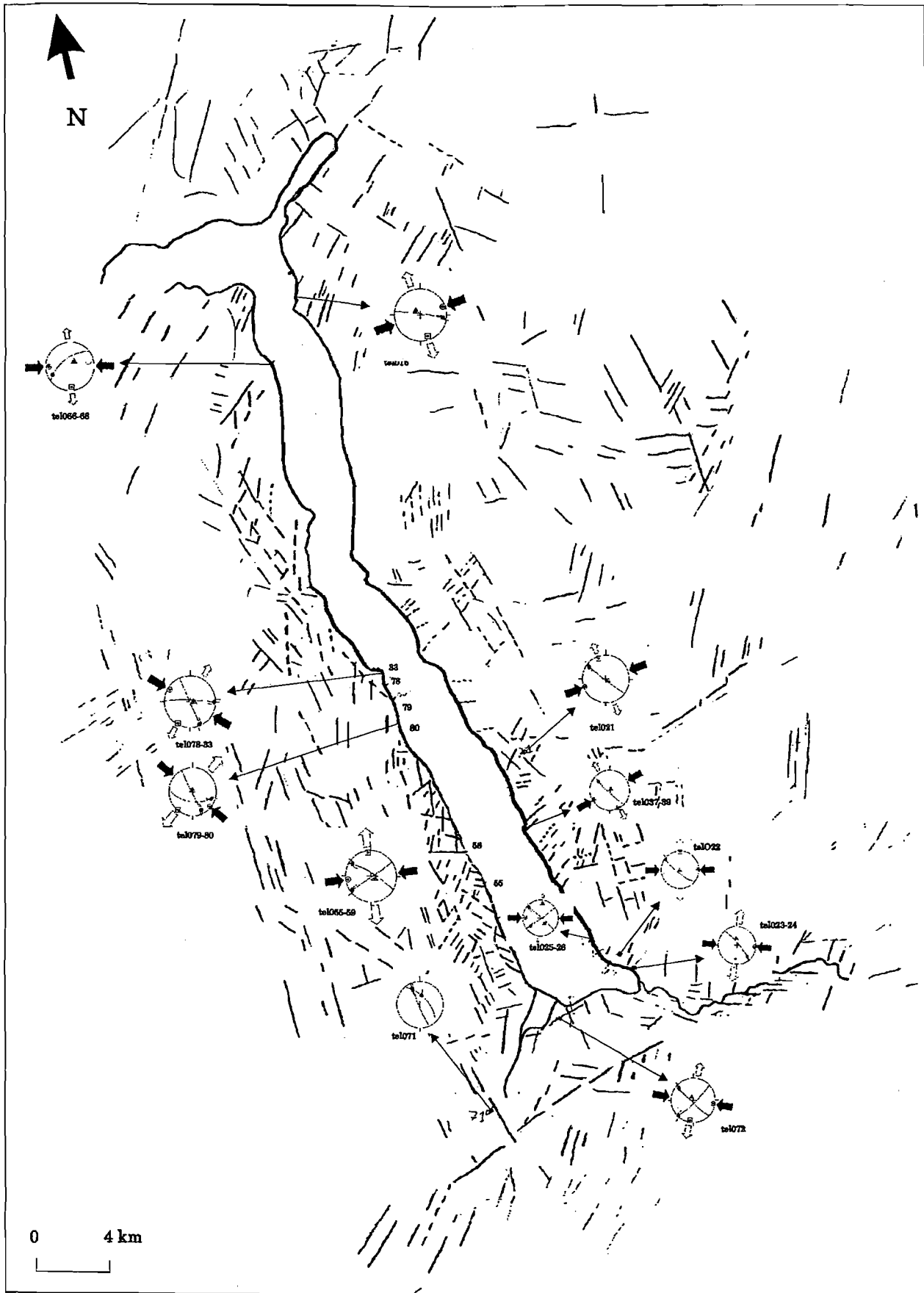


Fig. 5. - Fault kinematics. Relations between direction and sense of fault movements as observed in the field and lineament pattern derived from satellite images and aerial photographs. By this, the observed strain on meso- and macro scale is related to the principal stress direction derived from it.

of the outcrops of the NE walls and the height of the canyon walls is exceptional in the area.

The southern border of the lake seems to be marked by an E-NE trending fault system, which is expressed on the border as a line, and about 3 km to the south as a big lineament (figs. 4 and 5). Detailed field investigations in this area reveal an important strike-slip component in the movement, which could indicate a recent type of activation, or a reactivation of a pre-existing weakness zone, along which the recent fault system has developed.

Curved fault systems are observed both in the northwestern and southeastern part of the lake (fig. 4). They form so called 'loupe systems', which are block structures, downfaulted along the spoonlike faults. Several *en échelon* curved faults with unconsolidated breccia filling, were observed along the Bele terraces by means of submeridional high angle, fault breccia, filled movement planes. They are possibly related to the block morphology as observed on the aerial photographs. Also in the Chiri series, several step structures are observable, resulting from downfaulting of blocks due to the opening and possible rotation of the eastern lake shore. In the southern part of the Altyntauss massif, a small down faulted block, possibly similar to the Chiri loupe is present, but it is smaller and less clearly expressed.

In the north-west, a curved fault system seems to be present, similar to that from the Chiri loupe system. In both cases, there are indications that these structures developed along pre-existing weakness planes, since several faults in this zone were determined in the field as strike-slip faults, which are by definition incompatible with listric fault movements.

In the Teletsk shearzone, near its northern termination, a system of different curved normal faults was observed, with an unconsolidated breccia filling, indicating a system of normal extensional faults, dipping in the direction of the lake.

For most of the brittle structures (except for the NE trending lineaments which appear on both borders), two different geometries appear on both sides of the lake. In general, this may be attributed to a different rheology between the eastern and western borders.

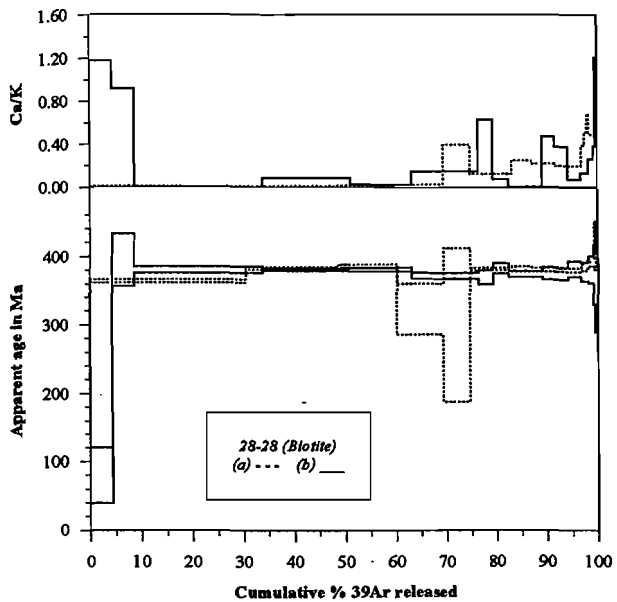
An analysis of the joints orientations shows that the direction of the most prominent sets, corresponds highly to the lineament orientations. So the joint pattern significantly accounts for the

local morphology of the region. It was also observed that many of the recent faults have orientations similar to the prominent joint sets.

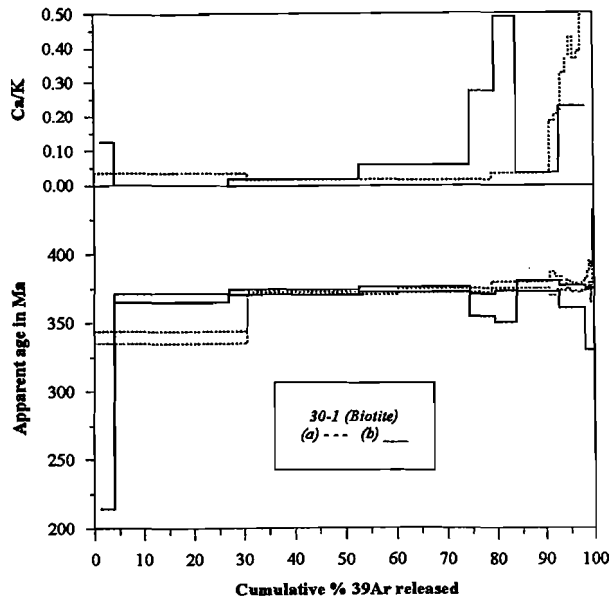
5.2. Paleostress analysis

Field investigation of fault kinematics was performed in the whole lake area, from its north-western termination up to about 30 km into the Chulyshman valley. The obtained data resulted in 27 reduced paleostress tensors determined by a stress inversion method. By this method, fault orientations and slip line orientations and senses of movements are used to calculate the four parameters of the reduced stress tensor. These are: σ_1 (principal compression direction), σ_2 (intermediate compression direction), σ_3 (minimal compression direction) and the ratio of principal stress differences $R = (\sigma_2 - \sigma_3) / (\sigma_1 - \sigma_3)$. These parameters allow to obtain the orientation and shape of the stress ellipsoid together with the orientation of the principal stress axes (Angelier, 1994). The TENSOR program (Delvaux, 1993) uses an improved version of the Right Dihedron method, developed by Angelier and Mechler (1977), along with a rotational optimisation method, minimising the deviation between the theoretical shear and the observed slip in a recursive way.

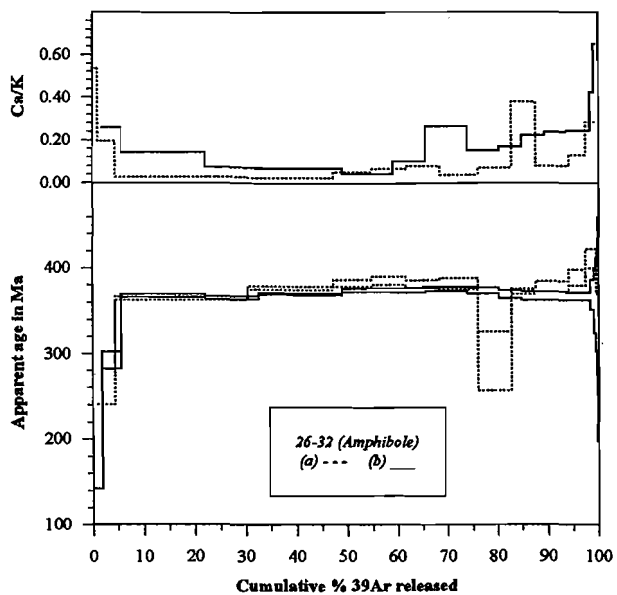
A compilation of the determined paleostress tensors is shown in table 1. Quartz mineralisations (slicken fibres) were observed on the slickensides. All the obtained tensors fit in a strike-slip to transpressional stress regime, but they show different orientations of the horizontal stress axes S_{Hmax} and S_{Hmin} . They also differ in mode of expression. Age estimations were generally difficult, because most of the outcrops were in the Proterozoic-Palaeozoic basement, but cross-cutting relations and a few outcrop sites located in late Pleistocene sediments allowed to constrain some phases. These distinctions resulted in the separation of three different stress stages (referred to as phase 1, 2 and 3). Phase 1 has a NW-SE principal compression direction, phase 2 shows E-W principal compression, and phase 3 accounts for the NNE-SSW direction of principal compression. The structures used for the paleostress determinations were mostly frictional grooves on fault planes (slickensides), extension joints (filled with quartz or calcite), and mineral lineations (in the brittle-ductile transition). The last type of kinematic structure was recognised only in one



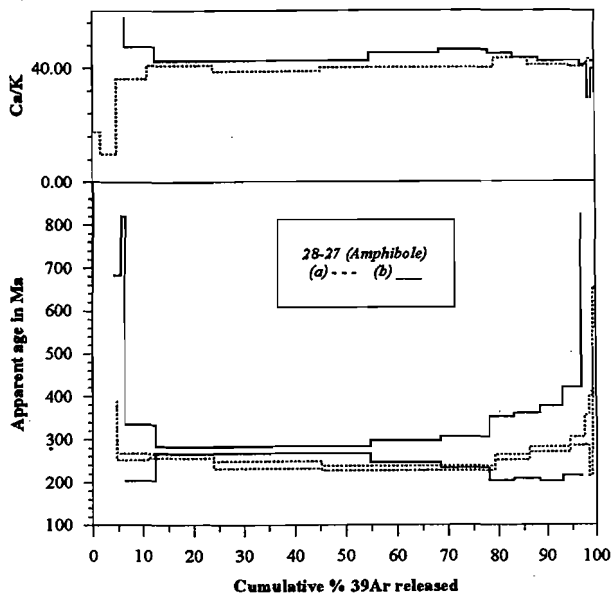
A.



B.



C.



D.

Fig. 6. - Stepwise heating age and Ca/K spectra for two sets of biotite (A and B) and two sets of amphibole (C and D). All samples were separated from mylonitic gneisses belonging to the Chiri-series (fig. 2). Apparent plateau ages are concordant for aliquots of A, B and C, with average values of respectively 380 ± 5 Ma; 375 ± 4 Ma and 378 ± 5 Ma. For sample D, aliquot (a) has an apparent plateau age of 236 ± 7 Ma, while aliquot (b) yields one single step age of 274 ± 9 Ma.

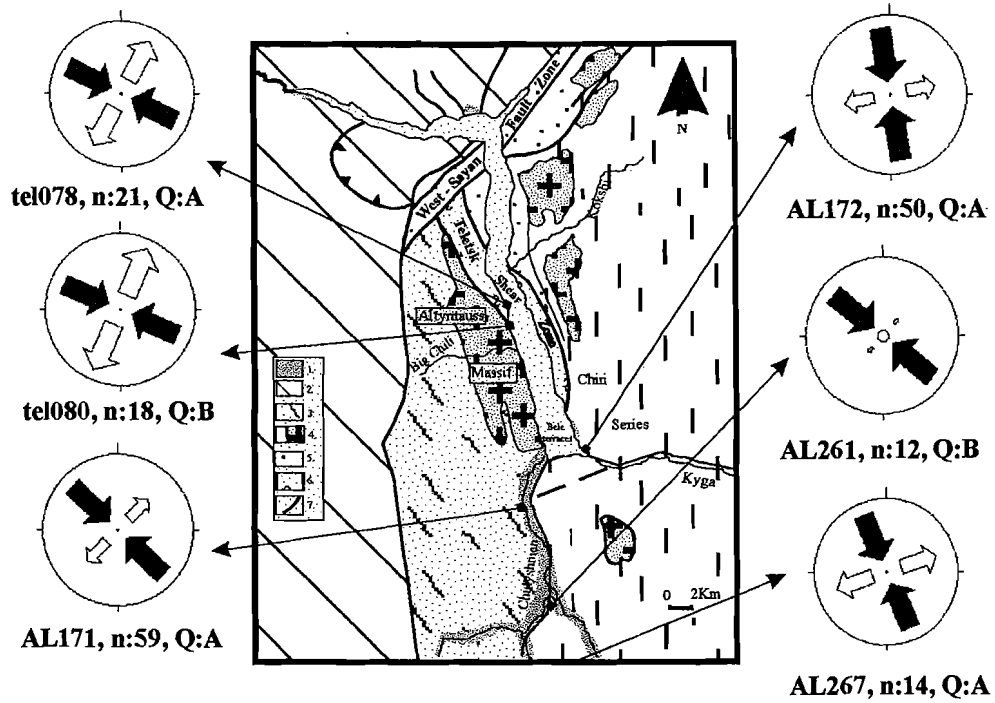


Fig. 7. – Paleostress ellipsoid orientation for phase 1.

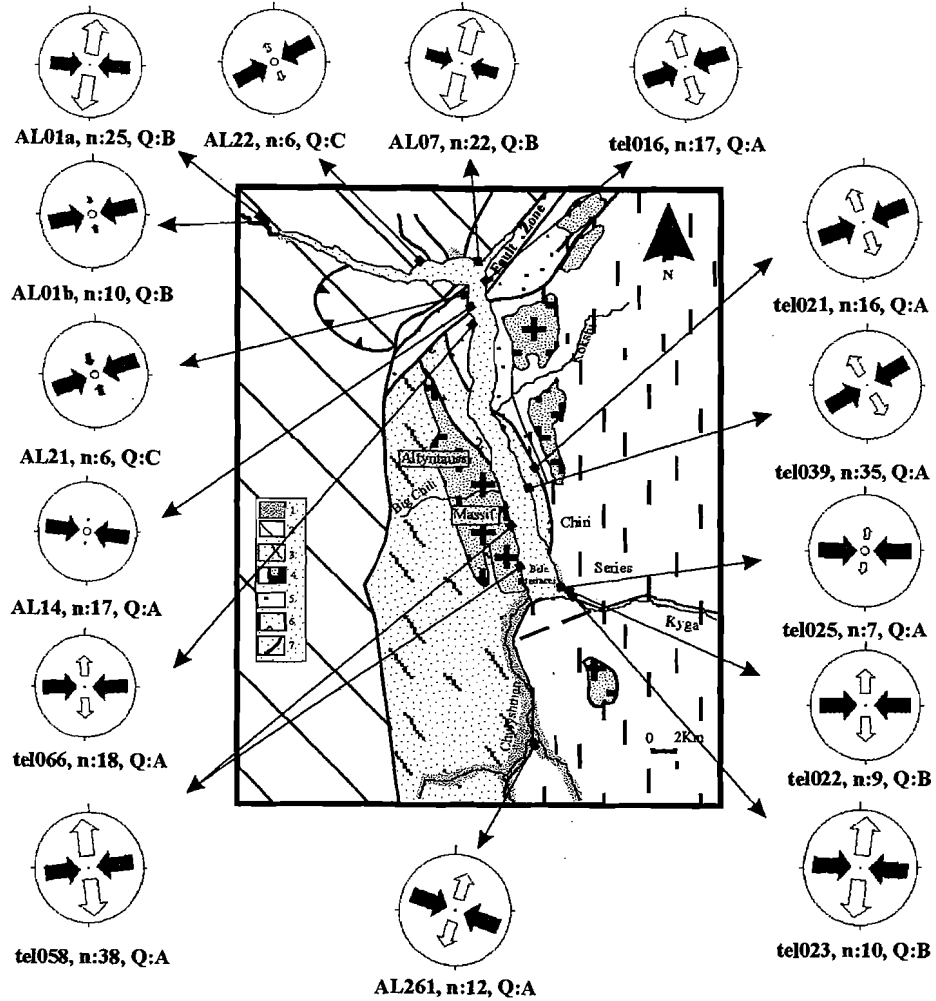


Fig. 8. – Paleostress ellipsoid orientation for phase 2.

tensor of 'phase 1'. The rest of the tensors were obtained from slickensides and extensional joints. The slickensides often had a mineral coating of brown hematite. Sometimes the sense of movement was determined according to the criteria described by Twiss and Moores (1994), Angelier (1994) and Hancock (1985). Table 2 describes the stress tensor derived from four earthquake focal mechanism from the Shapshal fault zone. The relation of the strain structures [statistical mean of the observed faults and slip directions as observed in the field, and the stress directions, derived from it] with the lineament pattern was acquired through comparison of the orientations and kinematics (fig. 5). This reveals in some parts of the area a clear correlation between the structures and the regional morphology. However, the kinematics observed in the field and those derived from remote sensing observations, did not seem to coincide. An important remark is that the normal faults, observed in the field and on the images, are not expressed by means of slickensides, but rather show brecciated fault planes. Strike-slip and inverse faults, instead, were very often expressed by slickensides.

6. INTERPRETATIONS

6.1. Geochronology

Table 3 shows that the four biotite aliquots (28-28 and 30-1) and the two amphibole aliquots of separate 26.32 yield apparent plateau ages within the range of $375\text{-}380 \pm 5$ Ma. Amphiboles have a higher closing temperature than biotite. In the present case there is no difference between the biotite ages and one amphibole age. Therefore, we may conclude that the metamorphic cooling of the Chiri must have been a very rapid process.

A similar situation was described by Dunné and Hancock (1994). Here hornblende and biotite from mylonite gneisses yielded similar $^{40}\text{Ar}\text{-}^{39}\text{Ar}$ cooling ages for amphibolite grade metamorphism. This is suggested to result from a rapid exhumation. Another comparable situation is described by Miller (Miller *et al.*, 1996) for a ductile shear zone. Phlogopite, hornblende and muscovite yielded similar $^{40}\text{Ar}\text{-}^{39}\text{Ar}$ ages, again interpreted as reflecting a period of fast cooling.

The mineral assemblages of the four measured samples as observed under the microscope, correspond to the upper amphibolite facies (see 4.2).

They were formed in an equilibrium state, and few secondary alterations were seen. The minerals are considered to result from a syntectonic recrystallisation. This most likely occurred at temperatures which are higher than the blocking temperature of biotite and amphibole.

The obtained apparent plateau ages (380 ± 5 Ma, Lower Devonian), similar on four biotites and two amphibole aliquots most likely reflects the time of metamorphic cooling of the gneisses. According to Buslov and Sintubin (1995), these gneisses are part of the zonal granite-gneiss domes, which were emplaced during the Devonian in an active continental margin environment. Later, in the late Permian, a collision resulted in the closure of the Palaeo-Asian ocean, affecting these granite-gneiss domes predominantly by strike-slip deformation.

The amphibole of sample 28-27 yields a younger apparent plateau age of about 260 ± 7 Ma (Lower Permian). Note that this separate is more enriched in the bigger greenish amphibole blasts of fabric 2 (see 4.2), which show a different orientation than the matrix amphiboles (fabric 1). This age could be attributed to a tectonic reactivation in low-grade conditions. Indeed, the staircase increase in apparent step ages of the spectrum may result from a mixing of grains with different apparent ages or from a loss of radiogenic argon by partial diffusion. The other samples, containing less grains of fabric 2, did not show any indication of this younger event, suggesting that the shear induced heating would be a local effect, restricted to narrow zones within the gneisses. More extensive data are needed to better illustrate these assumptions.

6.2. Paleostress

The significance of the three different paleostress phases is that the fault movement as observed in the field originated from one of these stress fields. Since all the calculated paleostress tensors display one of the three mean orientations (NW-, E- and NE-compression), we can suppose that these stress orientations are related to some event in the area, and do not result from local stress deviations at the scale of the outcrop. The important question of the age of activity of the three different phases (defined as changes in direction of principal stress axes) is difficult to answer, due to the lack of Permian, Mesozoic and Tertiary deposits in the region.

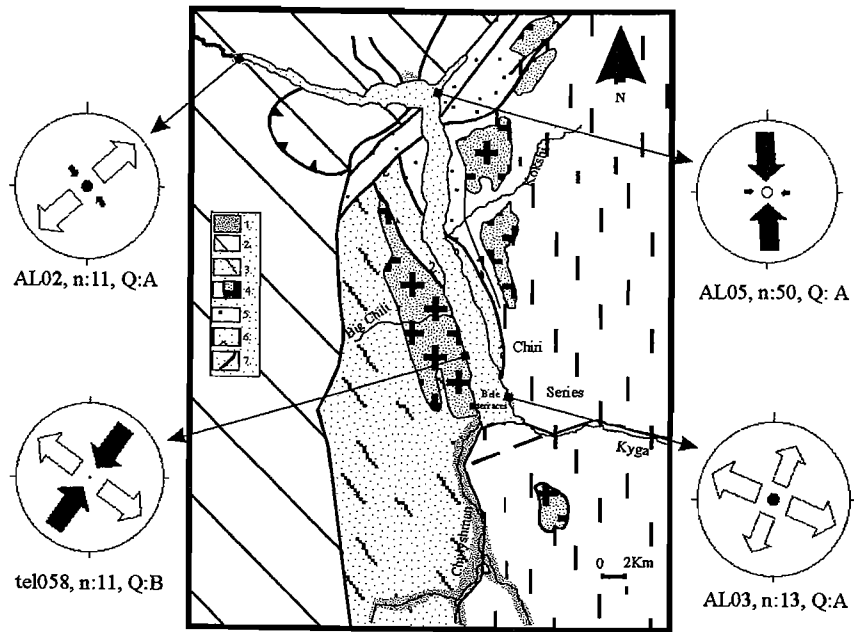


Fig. 9. - Paleostress ellipsoid orientation for phase 3.

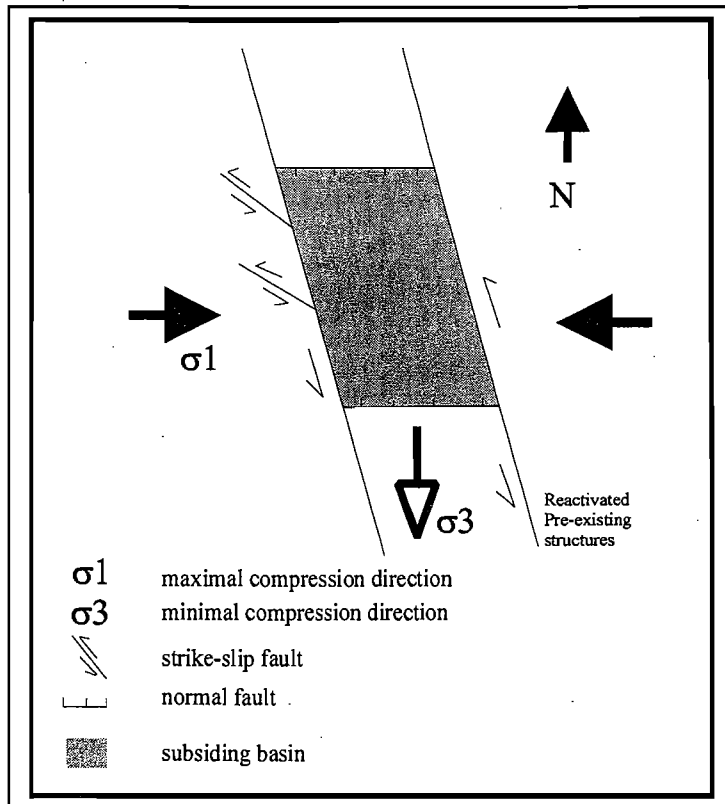


Fig. 10. - Model for the initial opening of the southern sub-basin in lateral principal compression. The lake's normal border faults acted as strike-slip faults during the initial opening in the Pliocene-Pleistocene. This resulted in the formation of a pull-apart basin, under a lateral compressive strike-slip stress regime. In a later phase, under submeridional compression, the northern lake segment opened due to lateral extension.

Only for the third phase (NNE-SSW compression in a strike-slip regime), we have a clear constraint for the age of movement, since it was derived from brittle structures in Quaternary sediments (fig. 9, Delvaux *et al.*, 1995a). The stress directions can be correlated to the general regime in which the lake is opening, in a submeridional principal compression direction. For the two other phases, we have to rely on interrelations of the phases, and on relations with morphology, regional structures and focal mechanisms.

In outcrop AL261 (figs. 7 and 8), a meta-breccia composed of Devonian rocks crops out, on which two orientations (NW compression and E-W compression) occur together. In this place, there is an obvious superposition of the E-W compression phase on the NW-SE compression phase. For this reason we call the latter orientation the older phase (phase 1), and the former orientation the younger phase (phase 2). In the Chulyshman valley (fig. 2), phase 1 and phase 2 do not affect glacial deposits, suggesting their pre-Quaternary age.

For 'phase 1' we have indications that it corresponds to a semi-ductile deformation stage. In outcrop AL261, this is derived from semi-ductile mineral lineations on a meta-breccia, associated to a thrustzone dipping east. This thrust is considered as being the southern (brittle) continuation of the ductile Teletsk shear zone, which also shows a dip to the east (Buslov and Sintubin, 1995). This could mean that phase 1 corresponds to an old tectonic regime, which was active close after or along with the ductile deformation of the basement in the area, i.e. during Palaeozoic tectonics. Five other calculated tensors correspond to this 'phase 1' tensor, both in orientation of the stress ellipsoid and in type of stress regime (fig. 7). However, they do not appear as semi-ductile mineral lineations, but more as real brittle slickensides with hematite coating. If these paleostress tensors, showing a compressive strike-slip regime with NW-SE principal compression, are associated to each other and do not result from blockrotations or block-tilts, they could reflect a Palaeozoic stress state of compressive and strike-slip deformation both in brittle and semi-ductile environments. Yet, two of the reduced paleostress tensors, derived from faults inside the Teletsk Shear Zone (fig. 7, tel078 and tel080) can also be related to a younger phase, with similar stress orientations, or to blockrotations.

The Teletsk shear zone is supposed to have undergone an important reactivation in the Quaternary. Therefore, the stress direction in this zone could be related to recent tectonics too. This idea is encouraged by the stress direction derived from earthquake focal mechanism of the Shapshal fault zone (table 2).

Fifteen paleostress tensors with a different orientation from 'phase 1' were grouped in 'phase 2' (fig. 8) on the basis of orientation, stress regime and slickenside style (mostly 'ridge in groove' striae, sometimes covered by a red or brownish epidote or hematite layer). The predominant part of these data were collected in faults that appear on aerial photographs and satellite images as pronounced lineations. Inside the faults of the Altyn-tauss massif, slip data were separated into two sub-sets, the first of which was classified in phase 2, and the second showed a principal compression direction congruous to the stress directions found in Quaternary sediments. Therefore, phase 2 is considered older than the recent stress state (phase 3), and younger than the semi-ductile (phase 1) situation.

Two possibilities are proposed:

6.2.1. Late Palaeozoic activity

There are several indications that this stress state corresponds to a tectonic phase which was active during the late Palaeozoic. In the Teletsk region, the faults intensely affect the Devonian intrusive granite-gneiss domes, and Devonian mylonitic gneisses (probably formed in the Teletsk shear-zone, which was formed under the phase 1 tectonic regime). This indicates a post-Devonian age. Structurally, thrust deformations affecting Carboniferous sediments are also easily seen in an E-W compressive stress regime.

More to the south-east of the Gorny-Altai terrain, the same phase affected Devonian granites and lava's (upper Katun river; Delvaux *et al.*, 1995a) and Carboniferous-Permian granites, along the Ursul river ($s_1=09/093$, strike-slip compressive regime, Delvaux, unpubl.). Also in the Kurai fault zone, in the Aktash-Chuya basin, a compressive strike-slip stress regime with latitudinal maximal principal stress direction was determined (Delvaux *et al.*, 1995a), affecting Middle Devonian to early Permian sediments, supporting the Permian dating of this phase. In a more general tectonic framework, it was stated (Dergunov, 1979; Mossakovsky and Dergunov, 1985; Buslov *et al.*,

1993; Sengör *et al.*, 1993 a.o.) that somewhere near the Carboniferous-Permian boundary, the final closure of the Palaeo-Asian Ocean occurred, with the collision of the Kazakhstan micro-continent and the Siberian continent. When this closure was established, the different geodynamic complexes achieved their present position. The Gorny-Altai block surmounted the sea level since the stop of the sedimentation at the end of the Lower Palaeozoic. Sedimentation in the Chuya-Kurai complex did not exceed the Lower Permian. The emersion resulted from the convergence of the two plates, with the closure of the oceanic basin at the end of the Palaeozoic. This indicates that as a result of this collision, and because the concerned terrains were situated at near-surface levels, important brittle deformations affected them at this time, which we determined as compressive and strike-slip regimes with a sub-latitudinal compression.

6.2.2. Pleistocene activity

There are indications that the formation of the Teletsk basin did not occur in one single stage, but that two phases of basin formation existed. In the first stage, only the southern basin was formed, because the West-Sayan fault zone, later inducing the opening of the northern part of the lake, was not active yet. The existence of such an early stage of basin formation is derived from seismological studies (Seleznyov *et al.*, 1996), which showed an abrupt decrease in sediment thickness in the central part of the lake, separating the northern from the southern sub-basin. The interpretation of the seismic records suggests a considerably younger age for the northern sediments, which were deposited only after the late Quaternary. Furthermore, seismic data revealed the existence of under water faults, striking parallel to the Teletsk fault zone (NW) in the south of the northern basin, and parallel to the West-Sayan fault zone (NE) in the northern part of the northern basin. They divide the northern part of the lake into several sub-basins, relatively displaced along the transverse faults.

It is possible that during the early stage (Pliocene-Pleistocene) of basin formation, when the southern part of the lake was formed, the border faults were activated under a 'phase 2' E-W transpressive stress regime, resulting in a sinistral movement of the 'Altyntauss type'. This idea is encouraged by observations made on NNW

striking lineaments (parallel to the lake border) and on NW oriented faults in the Altyntauss massif (fig. 8, tel058). They showed a clear sinistral sense of movement on their fault planes. In this sinistral movement of the leading faults (the present borders of the lake), the southern basin could have opened as a pull-apart basin (fig. 10). This would correspond to the early reactivation of the Teletsk shear zone. Later, extensional features developed in a submeridional compressive strike-slip regime when the northern basin was opened as imbrication of the transverse sub-basins, with the NW faults now moving in a dextral sense (phase 3). This last stage would be induced by the sinistral activation of the West-Sayan fault zone, also inducing the sinistral reactivation of the NE-trending faults (Altyntauss massif, phase 3). Due to the activation of strike-slip faults with opposite sense of movement (sinistral in the West-Sayan fault zone, dextral in the Teletsk fault zone and Shapshal fault zone), Teletsk Lake achieved its present shape and kinematics.

Possibly, the pre-existing NW trending sinistral transverse faults in the northern basin were reactivated as dextral strike-slip faults in the second stage of basin formation, since they are expressed in seismic profiles up to the sediment surface.

7. CONCLUSIONS

Dating of the ductile structures of the basement, using the $^{40}\text{Ar}-^{39}\text{Ar}$ stepwise heating technique, revealed similar cooling ages for two different geochronometers, biotite and amphibole, present in the fine-grained gneissic layers of the Chiri series, outcropping in the southeastern part of Lake Teletsk. These results indicate an early Devonian rapid cooling of the Chiri gneisses at about 380 ± 5 Ma, associated to the emplacement of the granite bodies within the West-Sayan terrain. This provides a maximum age constraint on the brittle events in this area, post-dating the exhumation process.

A second age, observed on two aliquots of the same Chiri gneisses, indicates an early Permian (260 ± 7 Ma) phase of heating, resulting in an Ar-clock reset. This heating is apparently restricted to narrow zones in the Chiri series. It is associated to a synkinematic recrystallisation of amphibole grains, according to an oblique fabric relative to the foliation of the gneisses. During the Permian, a

collision took place between the Siberian and Kazakhstan continents (Zoneshain *et al.*, 1990). In the Teletsk zone, this resulted in the formation of thrusts and strike-slip faults (Buslov and Sintubin, 1995), which could have a ductile shear component, represented by the Permian amphibole age.

Probably most brittle structures in the Teletsk region are post-dating the ductile process. Analysis of shear senses of brittle and semi-brittle structures resulted in the calculation of 27 reduced paleostress tensors for the Teletsk Lake area. They all fitted in a similar transpressional to strike-slip stress regime. Although clear age relationships remained rare, a separation of the tensors in three different phases was established through cross cutting- and stratigraphic relations. The first phase has a NW principal compression direction, the second phase an E-W principal compression, and the third phase a NNE principal compression.

Phase 1 corresponds to a post-ductile (i.e. post-early Devonian) Palaeozoic tectonic event, since it is expressed in semi-ductile mineral lineations. Cross cutting relations indicate that phase 2 post-dates phase 1, and stratigraphic relations indicate that phase 2 predates phase 3. Phase 3 is expressed in late Pleistocene (Würm) sediments and as reactivations of faults affecting the Altyntauss granites. For phase 2, two age possibilities are presented. The first possibility is attributed to Palaeozoic tectonics, possibly related to the Permian phase of local heating, put in a regional framework of collision-induced lateral compression. The second possibility is related to early Quaternary opening of the southern sub-basin, which could be explained by the formation of extensional duplexes with sinistrally moving leading faults.

Acknowledgments

The first author is financially supported by the IWT.

8. REFERENCES

Abrakhmatov, K. Y., Bradford, H.H., Hamburger, M.W., Herring, T.A., Makarov, V.I., Molnar, P., Panasyuk, S.V., Prilepin, M.T., Reilinger, R., Sadybakasov, I.S., Souter, B., Trapeznikov, Y.A., Tsurkov, V.Y. and Zubovich, A.V. (1996) - Relatively recent construction of the Tien Shan inferred from GPS measurements of present-day crustal deformation. - *Nature*, **384**, 450-453.

Angelier, J. (1994) - Fault slip analysis and paleostress reconstruction. - In : Hancock, P.L. (Ed.), *Continental Deformation*, Bristol, Pergamon Press, U.K., 53-100.

Angelier, J. and Mechler, P. (1977) - Sur une méthode graphique de recherche des contraintes principales également utilisable en tectonique et en sismologie : la méthode des dièdres droits. - *Bull. Soc. Géol. Fr.*, **7** (19), 1309-1318.

Berzin, N.A., Coleman, R.G., Dobretsov, N.L., Zoneshain, L.P., Xuchang, X. and Chang, E.Z. (1994) - Geodynamic map of the western part of the Paleasian Ocean. - *Russian Geology and Geophysics*, **35**, 5-12.

Buslov, M.M., Berzin, N.A., Dobretsov, N.L. and Simonov, V.A. (1993) - In : *Geology and Tectonics of Gorno Altai*, guide book for the 4th International Symposium of IGCP excursion, Novosibirsk : Russian Academy of Sciences, Siberian Branch.

Buslov, M.M. and Sintubin, M. (1995) - Structural evolution of the Teletsk zone, Altai-Sayan folded area Cenozoic. - *Russian Geology and Geophysics*, **36**, 10, 99-108.

Cobbold, P.R. and Davy, P.H. (1988) - Indentation tectonics in nature and experiment. 2. Central Asia. - *Bull. Geol. Inst. Univ. Uppsala, N.S.*, **14**, 143-162.

Delvaux, D. (1993) - The tensor program for paleostress reconstructions : examples from the east African and the Baikal rift zones. - *Terra nova*, Abstracts, **5**, p. 216.

Delvaux, D., Klerkx, J., Matton, C., Selegei, V., Theunissen, K. and Vysotsky, E. (1995a) - Evidences for active tectonics in Lake Teletskoye (Gorny Altai, South Siberia). - *Russian Geology and Geophysics*, **36**, 10, 109-122.

Delvaux, D., Theunissen, K., van der Meer, R. and Berzin, N. (1995b) - Dynamics and paleostress of the Cenozoic Kurai-Chuya depression of Gorny-Altai (South Siberia : tectonic and climatic control. - *Russian Geology and Geophysics*, **36**, 10, 26-45.

Dergunov, A.B. (1972) - Quaternary compression and extension structures in the eastern Altai. - *Geotectonics*, **3**, 99-110 (in Russian).

Dergunov, A.B. (1979) - Structure of the Caledonides and the development of the earth's crust in West Mongolia and the Altai-Sayan area, U.S.S.R. - *Proceedings of the IGCP Project 27, Caledonides in the USA*, 197-203.

Dobretsov, N.L., Berzin, N.A. and Buslov, M.M. (1995a) - Opening and tectonic evolution of the Paleo-

Asian Ocean. - *International Geology Review* 37, 335-360.

Dobretsov, N.L., Berzin, N., Buslov, M.M. and Ermikov, V.D. (1995b) - General aspects of the evolution of the Altai region and the interrelationships between its basement pattern and the neotectonic structural development. - *Russian Geology and Geophysics*, 36, 10, 3-15.

Dunné, W.M. and Hancock, P.L. (1994) - Paleostress analysis of small-scale brittle structures. - In : Hancock, P.L. (Ed.), *Continental Deformation*, Bristol Pergamon Press, 101-118.

Hancock, P.L. (1985) - Brittle microtectonics : principles and practice. - *Journal of structural Geology*, 7, 437-457.

Hess, J.C. and Lippolt, H.J. (1993) - Compilation of K-Ar measurements on HDB1 standard biotite. - *Bulletin of Liaison and Informations, IUGS subcommission on Geochronology*, 12, 19-23.

Kalugin, I., Bobrov, V., Scherbov, B., Klerkx, J. and Wartel, S. (1996) - Evolution of recent sedimentation of the Teletskoye Lake. - *INTAS Workshop: Continental Rift Tectonics and Evolution of sedimentary basins*, 55-57 (abstract).

Lukina, N.V. (1991) - The Teletskoye Lake young graben. - *Priroda*, 2, 56-64 (in Russian).

Miller, B.V., Dunning, G.R., Barr, S.M., Reaside, R.P., Jamiesson, R.A. and Reynolds, P.H. (1996) - Magmatism and metamorphism in a Grenvillian fragment : U-Pb and Ar-Ar ages from Blair River Complex, northern Cape Breton Island, Nova Scotia, Canada. - *GSA Bulletin*, 108, 2, 127-140.

Molnar, P. and Tapponnier, P. (1975) - Cenozoic tectonics of Asia : Effects of a continental collision. - *Science*, 189 (4201), 419-426.

Mossakovsky, A.A. and Dergunov, A.B. (1985) - The Caledonides of Kazakhstan, Siberia and Mongolia : a review of structure, development history and palaeotectonic environments. - In : Gee, D.G. and Sturt, B.A. (Eds.), *The Caledonide Orogen, Scandinavia and related areas*, JohnWiley & Sons Ltd., 1201-1215.

Seleznyov, V.S., Klerkx, J., Solovyov, V.M., Babushkin, S.M., Larkin, G.V. and Emanov, A.F. (1996) - Structure of sedimentary cover of the Teletskoye lake. - *INTAS Workshop : Continental rift Tectonics and Evolution of sedimentary basins*, 55-57 (abstracts).

Sengör, A.M.C., Natal'In, B.A. and Burtman, V.S. (1993) - Evolution of the Altai tectonic collage and palaeozoic crustal growth in Eurasia; - *Nature*, 364, 299-307.

Suess, E. (1901) - *Das Anlitz der Erde*. - Wien, Tempsky.

Tapponnier, P. and Molnar, P. (1979) - Active faulting and Cenozoic tectonics of the Tien Shan Mongolia and Baikal regions. - *Journal of Geophysical Research*, 84, B7, 3425-3459.

Twiss, J.R. and Moores, E.M (1992) - Introduction to faults. - In : *Structural Geology*, New-York, Freedman and Company, 51-73.

Zoback, M.L. (1992) - World stress map. - *Journal of Geophysical Research*, 97, 8, 11703-11728.

Zonenshain, L.P., Kuzmin, M.I. and Natapov, L.M. (1990) - *Geology of the USSR : a plate tectonic synthesis*. - Washington, DC, Amer. Geophys. Union, Geodynamic Monograph.

Table 1: Reduced Paleostress tensors for the Teletsk region

Teletsk Lake area, phase 1

Site	Lat.	Long.	Description	n	nt	σ_1	σ_2	σ_3	R	α	Q	R'
tel080	51 30	87 41	Northern end of Altyntauss massive	18	22	05/114	84/329	03/204	0.52	3.66	A	1.48
tel078	51 31	87 40	Southern end of Teletsk shearzone	21	37	06/132	37/040	53/227	0.25	9.9	A	1.60
AL172	51 21	87 50	Chiri series, gneisses	50	59	19/171	70/336	05/079	0.07	12.25	A	1.93
Weighed mean: 3 tensors				89		12/139	78/326	02/227	0.26			1.74

Chulyshman area, phase 1

Site	Lat.	Long.	Description	n	nt	σ_1	σ_2	σ_3	R	α	Q	R'
AL171	51 18	87 42	Balukchya area, mylonitic gneisses	59	64	00/134	78/223	12/044	0.04	14.09	A	1.96
AL261	51 12	87 48	River junction, metabrec. in thrustzone	12	16	20/129	10/223	69/337	0.38	12.15	B	2.38
AL267			Chulyshman canyon,	14	17	06/157	52/059	38/252	0.27	11.59	B	1.73
Weighed mean: 3 tensors				85		07/134	80/268	07/042	0.17			1.83

Northern-Teletsk, phase 2

Site	Lat.	Long.	Description	n	nt	σ_1	σ_2	σ_3	R	α	Q	R'
AL01	51 47	87 11	Arty Bash, older phase	10 ^(o)	51	03/258	02/348	86/110	0.60	5.25	B	2.60
AL01	51 47	87 11	Arty Bash area, younger phase	25 ^(o)	51	16/273	65/143	18/009	0.61	8.57	B	1.39
AL07	51 46	87 39	near West Sayan fault, metasediments	22	34	08/285	81/074	04/194	0.73	11.04	B	1.27
tel016	51 44	87 40	siliceous greenschists	17	18	09/070	72/310	15/162	0.30	0.05	A	1.70
AL10			Korby river	16	20	20/232	25/135	57/358	0.31	5.1	A	2.31
AL19				11	11	21/079	60/306	21/177	0.28	5.5	A	1.72
AL21	51 43	87 38	greenschists from Kockshi series	6	15	02/250	12/160	78/349	0.66	8.48	C	2.66
tel066	51 41	87 39	greenschists with quartz segregates	18	18	14/269	75/069	05/178	0.10	11.82	A	1.90
AL22	51 45	87 34	black slates	6	12	15/242	10/335	72/097	0.22	5.87	C	2.22
AL14	51 42	87 39	greenschists with quartz segregates	17	20	00/278	04/187	86/007	0.38	7.95	A	2.38
Weighed mean: 10 tensors				148		06/266	57/167	31/004	0.44			1.56

Southern Teletsk and Chulyshman valley, phase 2

Site	Lat.	Long.	Description	n	nt	σ_1	σ_2	σ_3	R	α	Q	R'
tel021	51 29	87 47	mylonitic greenschists	16	23	04/249	79/137	10/340	0.11	0.5	A	1.89
tel039	51 29	87 45	mylonites from Teletsk Shearzone	35	43	05/240	84/026	03/150	0.13	11.09	A	1.87
tel058	51 25	87 44	Altyntauss granitic massive	39 ²	50	10/262	77/120	08/353	0.53	4.81	A	1.47
tel022	51 22	87 49	Chiri gneisses	9	10	02/090	85/204	04/359	0.16	10.14	B	1.84
tel023	51 22	87 50	Chiri gneisses	10	15	06/094	62/353	27/187	0.50	12.38	B	1.50
tel025	51 22	87 49	Chiri gneisses	7	7	16/271	20/007	63/145	0.20	10.2	A	1.80
AL261	51 12	87 48	metabreccia in thrustzone	12	15	32/269	58/099	04/002	0.21	4.59	A	1.79
Weighed mean: 7 tensors				142		07/255	82/099	03/346	0.26			1.74

Altyntauss Massive, phase 3

Site	Lat.	Long.	Description	n	nt	σ_1	σ_2	σ_3	R	α	Q	R'
tel058	51 25	87 44	Altyntauss granitic massive	11 ²	50	01/036	83/134	07/386	0.48	4.81	B	1.47

Tensors derived from structures in Quaternary sediments

Site	Lat.	Long.	Description	n	nt	σ_1	σ_2	σ_3	R	α	Q	R'
AL02			Arty-Bash, Quaternary sands	18	20	83/198	03/317	06/048	0.73	9.4	A	1.27
AL03			Quaternary terrace	13	13	87/087	03/202	06/292	0.10	0.8	A	1.90
AL05			Airan Cape, Quat. tectonic breccia	50	86	09/357	29/092	59/250	0.58	11.1	A	2.58
Weighed mean: 4 tensors				101		02/179	69/274	21/088	0.94			1.06

Data show as: dip/azimuth

n: number of data used for tensor determination

nt: total number of data

$\sigma_1, \sigma_2, \sigma_3$, and R: see text

α : slip deviation

Q: quality of the tensor (A=good, B=medium, C=poor, D=not reliable (Delvaux, 1993))

R': stress regime: 0<R'<1: extensive; 1<R'<2: strike-slip; 2<R'<3: compressive

Table 2: Reduced Paleostress tensors derived from 4 Earthquake Focal mechanisms from the Shapshal fault zone (see fig.3)

Lat.	Long.	n	nt	σ_1	σ_2	σ_3	R	α	Q	R'
50.5-51.4	88.2-89.1	4	5	02/343	75/079	14/253	0.95	2.9	B	1.05

Table 3. – Analytical results from Ar-Ar stepwise heating measurements

Temp (°C)	⁴⁰ Ar/ ³⁹ Ar	³⁷ Ar/ ³⁹ Ar	³⁶ Ar/ ³⁹ Ar (10 ³)	³⁵ Ar/ ³⁹ Ar (10 ³)	³⁷ Ar/ ³⁸ Ar	³⁹ Ar Cum (%)	⁴⁰ Ar* (%)	⁴⁰ Ar*/ ³⁹ Ar	Ca/K	⁴⁰ Ar*/ ³⁷ Ar	Apparent Age ± 1 s.d. (Ma)
Sample 26-32											
<i>Aliquot (a) from Chiri, Teletsk, weight = 10.54 mg, J = 0.10048</i>											
700	27,81	0,10	88,99	27,46	3,52	4,45	5,50	1,53	0,19	15,81	258 ± 18
780	5,61	0,01	11,46	13,43	0,92	30,46	39,50	2,22	0,02	179,87	364 ± 2
840	2,42	0,01	0,38	11,36	1,02	47,33	95,54	2,31	0,02	199,38	376 ± 2
860	2,39	0,03	0,15	11,27	2,23	54,95	98,23	2,35	0,05	93,28	382 ± 4
880	2,38	0,03	0,03	11,43	2,76	61,73	99,75	2,37	0,06	75,09	385 ± 5
900	2,37	0,04	0,10	11,20	3,37	68,47	98,73	2,34	0,08	61,81	381 ± 4
930	2,37	0,02	0,12	10,91	1,61	76,01	98,65	2,34	0,04	133,13	381 ± 7
960	2,04	0,03	1,01	11,43	2,98	82,79	85,38	1,74	0,07	51,05	291 ± 35
980	2,48	0,19	0,73	6,58	28,43	87,60	92,05	2,28	0,38	12,19	372 ± 3
1030	2,38	0,04	0,21	11,43	3,27	94,09	97,39	2,32	0,07	61,96	378 ± 6
1080	2,45	0,06	0,22	11,37	5,63	97,38	97,50	2,39	0,13	37,36	388 ± 10
1130	2,56	0,14	0,09	10,61	13,18	99,56	99,28	2,54	0,28	18,15	410 ± 11
1230	125,02	21,66	238,88	331,53	65,32	99,92	44,29	55,37	1,81	2,56	377 ± 8
1340	384,76	131,43	1073,02	523,17	251,21	99,98	18,65	71,75	11,00	0,55	477 ± 47
<i>Aliquot (b) weight = 6.10 mg, J = 0.10048</i>											
570	41,44	~	137,84	34,86	~	1,83	1,57	0,65	~	~	114 ± 28
590	17,33	0,13	52,54	22,03	5,81	5,71	10,10	1,75	0,26	13,68	292 ± 10
620	4,64	0,07	8,08	13,28	5,28	22,06	48,37	2,24	0,14	31,99	367 ± 2
700	2,43	0,04	0,64	11,76	3,02	32,64	92,31	2,24	0,07	63,16	365 ± 2
760	2,32	0,03	0,17	11,60	2,89	49,09	97,84	2,27	0,07	67,76	369 ± 1
780	2,33	0,02	0,15	11,56	1,73	59,13	98,59	2,30	0,04	114,75	374 ± 2
800	2,33	0,05	0,15	11,75	4,22	65,63	98,26	2,29	0,10	46,12	374 ± 3
860	2,30	0,13	0,05	11,71	11,22	73,92	100,00	2,30	0,26	17,52	375 ± 2
880	2,31	0,07	0,08	11,65	6,34	80,20	99,21	2,29	0,15	30,99	373 ± 3
900	2,30	0,08	0,18	11,67	7,08	84,84	97,85	2,26	0,17	27,30	369 ± 5
930	2,31	0,11	0,22	11,55	9,56	89,42	97,20	2,24	0,22	20,33	367 ± 5
960	2,31	0,12	0,25	11,76	9,93	93,63	96,96	2,24	0,23	19,20	367 ± 5
980	2,33	0,12	0,33	11,66	10,39	98,29	96,06	2,24	0,24	18,48	366 ± 4
1000	2,40	0,21	0,50	11,74	17,90	99,08	93,67	2,25	0,42	10,72	368 ± 17
1030	2,42	0,32	0,72	12,01	27,00	99,45	91,26	2,20	0,65	6,80	361 ± 37
1050	2,47	0,57	1,03	12,27	46,33	99,71	87,93	2,18	1,14	3,83	357 ± 54
1130	2,61	1,01	1,77	12,94	77,78	99,89	80,20	2,09	2,01	2,08	344 ± 75
1410	3,44	1,59	4,93	13,45	118,49	100,00	57,89	1,99	3,19	1,25	329 ± 131
Sample 30-1											
<i>Aliquot (a) from Chiri, Teletsk, weight = 7.41 mg, J = 0.10048</i>											
750	9,31	0,02	24,52	15,75	1,11	30,72	22,06	2,06	0,04	117,12	339 ± 4
770	2,53	0,01	0,88	11,52	0,71	60,28	89,57	2,27	0,02	278,76	371 ± 1
800	2,34	0,01	0,22	11,39	0,64	78,90	97,56	2,29	0,01	312,50	373 ± 1
840	2,58	0,02	0,89	11,44	1,39	90,97	89,85	2,32	0,03	145,39	377 ± 2
860	2,38	0,09	0,20	11,50	8,05	92,04	97,34	2,32	0,19	25,07	378 ± 9
880	2,39	0,10	0,27	11,48	8,83	93,29	96,80	2,32	0,20	22,87	378 ± 5
900	2,38	0,16	0,31	11,54	13,94	94,26	96,45	2,30	0,32	14,30	375 ± 2
930	2,41	0,19	0,39	11,75	16,03	95,09	95,89	2,31	0,38	12,28	377 ± 3
960	2,41	0,21	0,37	11,57	18,46	95,79	95,16	2,29	0,43	10,73	375 ± 3
980	2,43	0,18	0,46	11,53	15,86	96,65	94,77	2,31	0,37	12,61	375 ± 3
1000	2,40	0,19	0,36	11,53	16,76	97,50	95,33	2,28	0,39	11,82	374 ± 3
1030	2,42	0,25	0,44	11,56	21,28	98,18	95,04	2,30	0,49	9,35	376 ± 3
1050	2,42	0,35	0,41	11,58	30,56	98,65	95,54	2,32	0,71	6,55	377 ± 5
1080	2,50	0,49	0,64	11,51	42,70	98,97	93,28	2,33	0,98	4,74	380 ± 7
1130	6,01	0,53	12,40	13,95	37,85	99,29	39,43	2,37	1,06	4,49	386 ± 8
1150	2,62	1,06	1,18	11,88	89,47	99,44	88,05	2,30	2,13	2,17	378 ± 14
1180	3,07	0,80	2,55	12,37	64,61	99,78	76,47	2,35	1,60	2,94	383 ± 7
1250	4,47	2,11	6,72	13,83	152,76	99,91	57,32	2,56	4,23	1,21	413 ± 18
1410	7,35	3,25	15,33	17,03	191,09	99,98	39,67	2,91	6,53	0,90	465 ± 33
1570	52,95	15,47	161,21	48,23	320,65	99,99	11,26	5,96	31,50	0,39	860 ± 180
1700	299,28	15,38	953,13	205,53	74,85	100,00	5,98	17,91	31,20	1,16	1880 ± 129
<i>Aliquot (b) weight = 4.61 mg, J = 0.10048</i>											
6	20,58	0,06	66,09	25,36	2,44	3,97	5,23	1,08	0,12	17,40	185 ± 29
7	6,92	~	15,75	14,70	~	27,03	32,55	2,25	~	~	368 ± 3
8	2,40	0,01	0,39	11,53	0,79	52,86	95,18	2,29	0,02	252,40	372 ± 2
8	2,40	0,03	0,35	11,56	2,47	74,68	95,71	2,29	0,06	80,24	374 ± 2
9	2,44	0,14	0,80	11,85	11,44	79,73	90,58	2,21	0,27	16,28	362 ± 8
9	2,50	0,24	1,03	11,91	20,51	84,03	88,15	2,20	0,49	9,00	361 ± 11
10	2,44	0,02	0,45	11,69	1,50	92,89	94,47	2,31	0,04	131,81	376 ± 4
11	2,43	0,11	0,64	11,77	9,70	98,16	92,42	2,25	0,23	19,69	368 ± 8
14	2,92	0,41	2,67	12,36	33,17	99,96	73,05	2,13	0,82	5,20	352 ± 22

Due to small concentration of Ca in the separates, ³⁷Ar ratios are omitted (-).

Temp (°C)	⁴⁰ Ar/ ³⁹ Ar	³⁷ Ar/ ³⁹ Ar	³⁶ Ar/ ³⁹ Ar (10 ³)	³⁸ Ar/ ³⁹ Ar (10 ³)	³⁷ Ar/ ³⁸ Ar	³⁹ Ar Cum (%)	⁴⁰ Ar* (%)	⁴⁰ Ar*/ ³⁹ Ar	Ca/K	⁴⁰ Ar*/ ³⁷ Ar	Apparent Age ± 1 s.d. (Ma)
--------------	------------------------------------	------------------------------------	--	--	------------------------------------	-----------------------------	--------------------------	-------------------------------------	------	-------------------------------------	-------------------------------

Sample 28-27

Aliquot (a) from Chiri, Teletsk, weight = 13.69 mg, J = 0.10048

400	3368,72	15,53	11117,32	2000,00	7,77	0,08	2,64	88,83	31,60	5,72	3750 ± 511
780	324,86	8,67	1087,57	231,36	37,48	1,56	1,21	3,93	17,50	0,45	484 ± 202
880	6,53	4,80	14,87	18,64	257,68	4,77	35,31	2,31	9,68	0,48	378 ± 10
1000	4,41	17,60	11,98	18,39	956,96	10,89	34,01	1,50	35,90	0,09	258 ± 7
1080	3,07	19,95	7,72	14,81	1347,11	24,07	49,00	1,51	40,70	0,08	260 ± 5
1130	2,74	18,80	5,54	13,81	1361,43	45,33	65,32	1,79	38,40	0,10	240 ± 8
1180	2,62	19,53	5,40	13,23	1476,64	79,27	66,04	1,73	39,80	0,09	232 ± 5
1230	3,24	21,14	8,54	14,52	1455,97	86,34	45,92	1,49	43,30	0,07	257 ± 6
1270	3,95	19,85	10,35	14,57	1362,43	94,71	40,54	1,60	40,70	0,08	275 ± 6
1300	4,73	19,63	12,53	15,47	1268,71	97,78	36,41	1,72	40,10	0,09	293 ± 10
1340	10,32	20,15	30,97	20,15	1000,00	98,64	18,26	1,88	41,10	0,09	320 ± 34
1370	105,75	20,85	353,42	79,18	263,32	99,23	1,70	1,80	42,70	0,09	306 ± 91
1570	39,93	20,51	125,64	38,46	533,33	100,00	9,27	3,70	41,90	0,18	580 ± 72

Aliquot (b) weight = 9.55 mg, J = 0.10048

800	12,31	11,86	32,48	34,92	339,68	3,45	25,32	3,12	24,00	0,26	497 ± 492
860	8,13	15,38	22,31	27,94	550,34	4,37	25,77	2,09	31,30	0,14	350 ± 555
900	6,88	22,05	20,70	26,37	835,98	5,61	22,84	1,57	45,10	0,07	270 ± 412
960	5,23	27,86	14,81	27,34	1019,00	6,50	35,61	1,86	57,60	0,07	319 ± 500
1000	3,13	23,20	8,14	16,70	1389,53	12,42	49,69	1,55	47,50	0,07	268 ± 65
1080	2,62	20,65	5,96	14,13	1461,54	54,79	61,14	1,60	42,20	0,08	274 ± 9
1130	2,69	21,88	6,49	14,31	1529,24	68,55	58,23	1,57	44,90	0,07	270 ± 25
1170	2,73	22,50	6,67	14,64	1536,59	78,22	57,30	1,57	46,00	0,07	269 ± 36
1210	2,91	21,87	7,05	14,74	1484,13	83,14	55,42	1,61	44,70	0,07	277 ± 74
1250	3,42	21,07	8,57	15,19	1387,32	88,53	48,44	1,66	43,20	0,08	283 ± 76
1290	3,40	20,52	8,32	15,36	1336,00	93,21	49,46	1,68	42,00	0,08	288 ± 87
1320	3,57	20,80	8,30	16,08	1293,58	97,12	52,48	1,87	42,40	0,09	317 ± 102
1400	7,26	19,92	16,05	20,16	988,00	98,54	44,39	3,22	40,80	0,16	517 ± 304
1570	20,60	14,23	50,34	30,74	462,88	99,40	30,07	6,19	28,90	0,44	882 ± 466
1700	95,10	19,13	309,62	84,23	227,17	100,00	4,50	4,28	39,10	0,22	656 ± 784

Sample 28-28

Aliquot (a) from Chiri, Teletsk, weight = 7.13mg, J = 0.10048

750	5,56	0,01	11,30	13,17	0,47	30,49	39,86	2,22	0,01	359,14	364 ± 2
770	2,45	0,01	0,31	11,30	0,57	48,63	95,58	2,34	0,01	361,20	382 ± 2
800	2,42	0,01	0,20	11,31	0,84	60,32	97,64	2,37	0,02	249,29	385 ± 3
850	2,11	0,01	0,55	11,69	1,09	69,41	92,40	1,95	0,03	153,58	322 ± 38
860	2,49	0,19	2,38	10,03	1,25	74,75	72,25	1,80	0,39	9,33	299 ± 112
880	2,45	0,06	0,36	11,47	5,19	83,15	95,88	2,35	0,12	39,45	381 ± 2
900	2,70	0,12	1,22	11,62	10,46	87,06	86,86	2,35	0,24	19,32	381 ± 4
930	2,55	0,11	0,75	11,37	9,32	91,57	91,28	2,32	0,21	21,94	380 ± 3
960	2,51	0,10	0,66	11,48	8,37	96,84	92,44	2,32	0,19	24,20	379 ± 3
1080	62,94	4,55	21,93	285,93	15,90	97,45	89,93	56,60	0,38	12,45	383 ± 5
1100	62,71	6,05	21,70	273,70	22,10	97,93	90,04	56,47	0,51	9,33	384 ± 6
1130	15,56	1,58	14,64	56,59	27,93	98,33	72,50	11,28	0,67	7,14	389 ± 7
1150	15,67	1,14	15,19	56,45	20,22	99,31	71,86	11,26	0,49	9,86	388 ± 3
1170	13,50	1,52	37,09	19,69	77,09	99,71	18,98	2,56	3,04	1,69	414 ± 34
1210	3,00	0,60	8,03	4,34	137,66	99,91	21,59	0,65	5,65	1,08	483 ± 64
1300	16,84	3,82	47,37	23,46	162,99	99,95	17,73	2,99	7,69	0,78	476 ± 73

Aliquot (b) weight = 7.60 mg, J = 0.10048

570	19,28	0,59	63,79	24,76	23,85	4,32	2,33	0,45	1,18	0,76	80 ± 41
620	7,20	0,46	16,15	14,75	31,13	8,70	33,74	2,43	0,92	5,29	394 ± 38
730	2,38	~	0,14	11,87	~	33,95	98,27	2,34	~	~	380 ± 4
780	2,38	0,04	0,14	11,54	3,59	51,17	98,20	2,34	0,08	56,36	380 ± 2
840	2,37	0,01	0,12	11,55	0,87	63,20	98,28	2,33	0,02	232,65	380 ± 2
860	2,36	0,07	0,32	11,50	6,11	76,42	96,06	2,26	0,14	32,19	371 ± 4
880	2,45	0,31	0,71	12,24	25,21	79,27	91,90	2,25	0,62	7,29	369 ± 11
900	2,35	0,04	0,03	11,65	3,07	82,53	100,00	2,35	0,07	65,55	382 ± 7
930	2,35	~	0,21	11,57	~	89,25	97,36	2,29	~	~	374 ± 4
960	2,41	0,23	0,40	11,58	20,09	91,65	95,32	2,30	0,47	9,87	375 ± 9
980	2,37	0,18	0,27	12,08	15,25	94,13	96,65	2,29	0,37	12,42	374 ± 9
100	2,36	0,03	0,09	11,70	2,72	96,73	98,80	2,33	0,06	73,29	381 ± 11
1030	2,40	0,06	0,27	11,62	5,31	98,19	96,39	2,31	0,12	37,40	377 ± 13
1050	2,44	0,13	0,39	11,63	11,10	99,19	95,59	2,33	0,26	18,08	380 ± 19
1080	2,50	0,19	0,72	11,71	16,03	99,65	91,57	2,29	0,38	12,18	373 ± 43
1130	2,83	0,60	1,93	12,13	49,52	99,89	80,00	2,26	1,20	3,77	370 ± 80
1210	4,46	2,55	9,20	14,94	170,43	99,94	38,92	1,73	5,11	0,68	291 ± 459
1410	7,66	4,15	20,06	21,74	190,91	99,97	22,89	1,75	8,33	0,42	294 ± 685

Due to small concentration of Ca in the separates, ³⁷Ar ratios are omitted (-).